J Fluoresc (2014) 24:745–750
DOI 10.1007/s10895-013-1347-y

ORIGINAL PAPER

Fluorescence Spectroscopy and Confocal Microscopy of the Mycotoxin Citrinin in Condensed Phase and Hydrogel Films

Milena H. Lauer · Marcelo H. Gehlen · Karen de Jesus · Roberto G. S. Berlinck

Received: 25 November 2013 / Accepted: 27 December 2013 / Published online: 10 January 2014

Abstract The emission spectra, quantum yields and fluorescence lifetimes of citrinin in organic solvents and hydrogel films have been determined. Citrinin shows complex fluorescence decays due to the presence of two tautomers in solution and interconversion from excited-state double proton transfer (ESDPT) process. The fluorescence decay times associated with the two tautomers have values near 1 and 5 ns depending on the medium. In hydrogel films of agarose and alginate, fluorescence imaging showed that citrinin is not homogeneously dispersed and highly emissive micrometer spots may be formed. Fluorescence spectrum and decay analysis are used to recognize the presence of citrinin in hydrogel films using confocal fluorescence microscopy and spectroscopy.

Keywords Citrinin · Natural product · Emission decay · Fluorescence imaging

Introduction

Citrinin is a common mycotoxin produced by filamentous fungi belonging to the genera *Penicillium*, *Monascus* and *Aspergillus*. Citrinin may be found in contaminated grains and food which have been infected by harmful fungal strains. Citrinin control and detection in food became relevant aspect of quality control because citrinin is considered a toxin that may cause serious liver, kidney and nervous system health problems [1]. Chemical analysis of citrinin has been based on chromatographic techniques more recently associated with mass spectrometry detection [1–4]. It is also analyzed using bioassay protocols [5]. Considering that citrinin usually occurs in very low concentrations in contaminated food samples, its recovery using specific adsorption techniques is a challenging task, which may lead to unreliable quantitative analysis. Polymeric matrices and nanoparticles are usually used for citrinin adsorption prior to analysis [6].

Although the fluorescence of citrinin has been previously described and frequently used in liquid chromatographic coupled to fluorescence detectors [1, 4, 5], citrinin emission properties have been less explored. Recently, the fluorescence properties of citrinin complexed with β-cyclodextrin have been described by Wang and co-workers [7].

There is no method of citrinin analysis with good performance based on its self-emission detected by microscopy. Herein we report the combination of time-resolved fluorescence spectroscopy and confocal microscopy of prepared samples containing traces of citrinin dispersed in hydrogel films as a strategy to be used in citrinin analysis.

Experimental part

Citrinin was isolated from *Penicillium citrinum* growth medium using the following procedure. *P. citrinum* was grown in five 500 mL Schott flasks containing 250 mL of malt 2 % media during 15 days, in still mode at 25 °C. At day 14, the culture medium of each Schott flask was extracted with 250 mL of ethyl acetate with occasional shaking over 2 days. Then, the mixture of solvent and growth media were filtered through a celite pad. The filtered mixture was partitioned in a separatory funnel to afford two fractions, the ethyl acetate and the aqueous fraction. The aqueous fraction was discarded.

The ethyl acetate fraction (422.7 mg) obtained after the solvent evaporation was dissolved in 1:1 H_2O:MeOH, and applied onto a silica-gel C_{18} reversed-phase cartridge (10 g)

M. H. Lauer · M. H. Gehlen (✉) · K. de Jesus · R. G. S. Berlinck
Instituto de Química de São Carlos – Universidade de São Paulo, São Carlos, Brazil
e-mail: marcelog@iqsc.usp.br

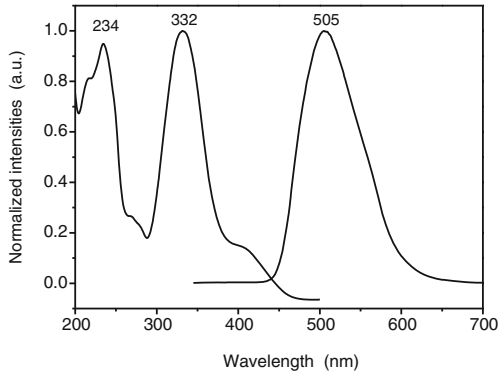

Fig. 1 Electronic absorption and emission spectra of citrinin in acetonitrile, λ_{exc}=332 nm

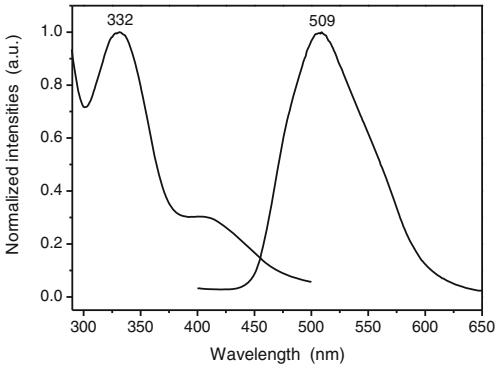

Fig. 3 Electronic absorption and emission spectra of citrinin in THF, λ_{exc}=332 nm

and eluted with a gradient of H_2O in MeOH (from 50:50 to MeOH 100 %).

The second fraction obtained from the previous separation (57.8 mg) was purified by HPLC using an Inertsil ODS-SP column (250×4.6 mm, 5 μm). The separation was performed in an isocratic mode with 6:2:2 H_2O:MeOH:MeCN, each solvent containing 0.1 % formic acid. The HPLC separation was monitored at λ_{max} 254 nm, and provided 10 mg of pure citrinin. The compound identity was established by ^{1}H NMR, ^{13}C NMR and mass spectrometry analysis, and by comparison with literature data [8, 9].

The solvents used (2-propanol, acetonitrile and THF) were of HPLC grade and dried in 4 Å molecular sieves prior to use. Polyvinylpirrolidone (PVP, M_w=29,000 gmol^{-1}, from Sigma-Aldrich) solution was prepared at 2 % mass in 2-propanol (from J. T. Baker). One equivalent of calcium chloride was added to sodium alginate (from Sigma-Aldrich) in order to form calcium alginate. The solutions of calcium alginate and agarose (from Sigma-Aldrich) were prepared in Milli-Q water at 0.1 and 1 % mass concentration. These systems were stirred at 60 °C for 2 h. Citrinin aliquots from a stock solution of 1.0×10^{-5} molL^{-1} in 2-propanol were added to the prepared matrix solutions to give a final concentration in the range of 10^{-7}–10^{-8} molL^{-1}. After addition of citrinin, the samples were stirred over 30 min and the respective hydrogel films were prepared by spin coating over clean glass slits # 1.5.

Electronic absorption spectra were determined in solution with a Jasco V-630 spectrophotometer and the corresponding emission spectra were obtained using a Hitachi F-4500 spectrofluorimeter with samples at 298 K. Fluorescence decays were measured by time-correlated single-photon counting technique (TCSPC) with excitation at 400 nm by frequency doubling the 150 fs laser pulses of a Ti-Sapphire Mira 900 laser pumped by Verdi 5 W (Coherent). The fluorescence decays were collected in magic angle mode (54.7°) using Glan-Laser polarizers (Newport), with 10^4 peak counts and time increment of 25 ps per channel. A Peltier cooled PMT-MCP (Hamamatsu R3809U-50) was used as photon detector, and the typical instrument response function (irf) of the home-made spectrometer was about 40 ps at fwhm. Decays were recorded with the TC900 Edinburgh counting board and analyzed with its FAST software.

Fluorescence images were obtained using a plate scanning confocal microscope setup. The lab-made instrument is based on a microscope (Olympus IX71) with a digital piezoelectric controller and stage (PI, E-710.3CD and P-517.3CD) for nanometric sample scanning. The excitation at 405 nm from a CW diode laser (Coherent Cube) was converted into a circularly polarized laser beam using zero-order quarter-

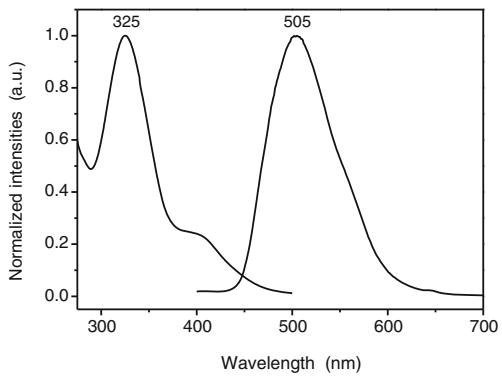

Fig. 2 Electronic absorption and emission spectra of citrinin in 2-propanol, λ_{exc}=325 nm

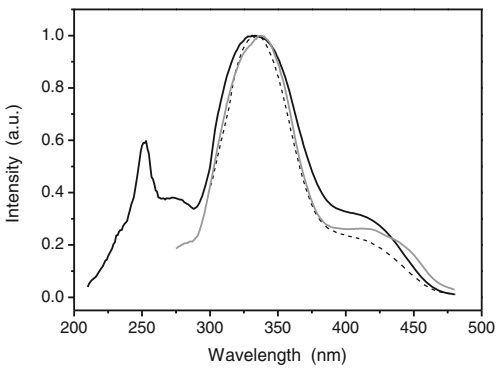

Fig. 4 Excitation spectra of citrinin in acetonitrile (*black line*), 2-propanol (*dash line*) and THF (*gray line*), λ_{em}=500 nm. The excitation maxima were 331, 334, and 336 nm, respectively

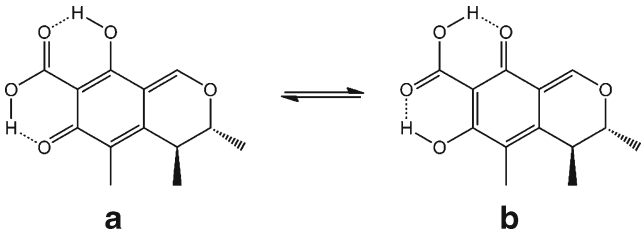

Fig. 5 Tautomeric forms of citrinin: *p*-quinone (**a**) and *o*-quinone (**b**)

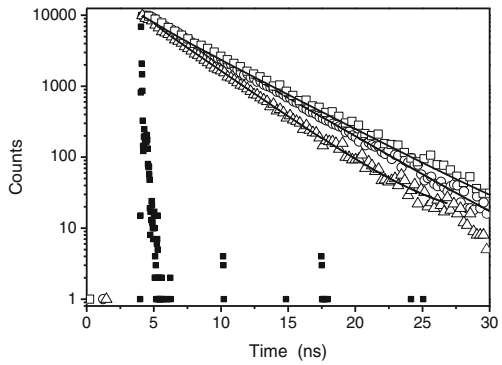

Fig. 6 Fluorescence decays of citrinin in (*white square*) isopropanol, (*white circle*) acetonitrile and (*white triangle*) THF. (*black square*) irf, λ_{exc}=400 nm and λ_{em}=500 nm

Table 1 Time-resolved data of citrinin in different solvents

Solvent	τ_1 (ns)	τ_2 (ns)	$\tilde{a}_1$	f_1 (%)	f_2 (%)	χ^2
2-propanol	1.52	4.45	0.16	6	94	1.21
Acetonitrile	1.72	4.00	0.11	5	95	1.18
THF	0.76	3.31	0.17	4	96	1.12

$\tilde{a}_1$ is the normalized amplitude ($\tilde{a}_1+\tilde{a}_2=1$). Decay times ($\tau_{1,2}$) and relative fraction of the components ($f_{1,2}$). chi-square of the fitting (χ^2)

wave plates (Del Mar Photonics) and focused on the sample with an objective (Olympus, UPLFLN 60X NA=1.35). The emission signal was separated from the laser excitation beam using a dichroic cube (Chroma, z405lp) and notch filter (Semrock, NF02-405U-25). Photons were counted using an avalanche photodiode point detector (Perkin Elmer, SPCM-AQR-14) aligned with a 50 μm pinhole in the confocal line. Transistor-transistor logic (TTL) detector signals were registered in a counter/timer PCI card (NI 6601) and transferred to a personal computer for 2D plotting using a scanning control program written in C#. Fluorescence images covering a square region of 60×60 μm with a pixel size of 200 nm were recorded using false-color mapping, reaching the best contrast enhancement according to the difference in intensity of the fluorescence signal. Hereafter, the position of a given emission spot was repositioned for decay measurements and emission spectrum determinations. In time resolved experiments, the frequency doubled light pulses from the Ti: sapphire laser (Mira 900) system at 400 nm was coupled to the microscope for sample excitation. Fluorescence decays were measured by TCSPC technique using a counting board (Becker & Hickl, 140) with start laser pulses triggered by a photodiode (PicoQuant TDA 200). Decays were analyzed with exponential models without deconvolution using the FAST software (Edinburgh Instruments). Emission spectra were obtained using a spectrometer (Maya 2000 Pro, Ocean Optics) coupled with a fiber to the binocular side port of the Olympus IX71 microscope. A long pass filter (Thorlabs, cut-off wavelength of 450 nm) was used to block the scattering light from the excitation.

Results and Discussions

In acetonitrile, a polar aprotic solvent, citrinin has a strong absorption band centered at 332 nm and a shoulder near 400 nm that allow easy laser excitation in the near UV region. Its fluorescence spectrum has a large Stokes shift and the emission maximum appears at about 500 nm depending on the solvent medium. The electronic absorption and emission

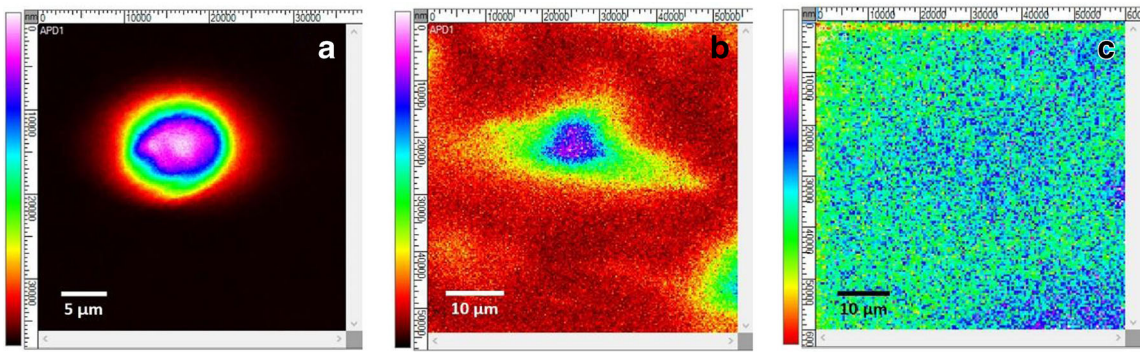

Fig. 7 Confocal fluorescence images of citrinin emission at 10^{-7} mol/L in different hydrogel films. Agarose 1 % (**a**), alginate 0.1 % (**b**) and PVP 2 % (**c**)

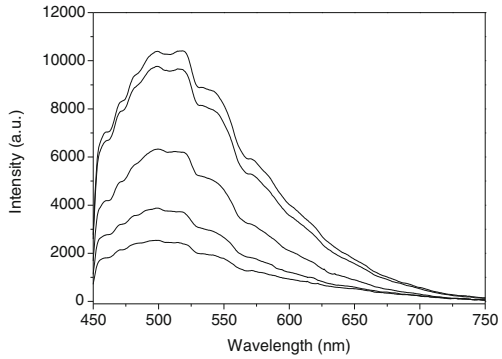

Fig. 8 Emission spectra of citrinin 1.0×10^{-7} M in calcium alginate 0.1 % film in different regions (from the center emission spot to the borders, see Fig. 7b). Partial waving of the emission spectra is due to the effect of optical filters used

Table 2 Time-resolved parameters of citrinin 1.0×10^{-7} M in hydrogel films

Hydrogel film	Decay[(a)]	τ_1 (ns)	τ_2 (ns)	$\tilde{a}_1$	f_1 (%)	f_2 (%)	χ^2	Counts
Agarose 1 %	1	1.67	6.11	0.61	33	67	1.02	3,000
	2	1.43	5.21	0.65	30	70	1.04	2,000
	3	1.68	5.70	0.64	36	64	1.02	2,000
Alginate 0.1 %	1	1.31	4.74	0.59	28	72	1.03	3,000
	2	1.01	4.42	0.78	45	55	1.03	3,000
	3	1.50	5.97	0.70	37	63	0.97	2,000

(a) 1, 2, 3 represent different regions of the same micrometric emission spot. $\tilde{a}_1$ is the normalized amplitude ($\tilde{a}_1+\tilde{a}_2=1$). Decay times ($\tau_{1,2}$) and relative fraction of the components ($f_{1,2}$). chi-square of the fitting (χ^2)

spectra of citrinin in acetonitrile are given in Fig. 1. Figures 2 and 3 show the absorption and emission of citrinin in 2-propanol and THF, respectively. The excitation spectrum of citrinin with emission recorded at 500 nm resembles the absorption profiles with a maximum near 330 nm and a second low intensity band at about 420 nm as illustrated in Fig. 4. The emission quantum yields of citrinin were calculated as 0.06 and 0.02 in acetonitrile and 2-propanol, respectively.

Neutral citrinin can form two major tautomeric species corresponding to the chemical structures illustrated in Fig. 5 [10–12]. A third isomeric form due to keto-enol conversion may be also formed but it is less stable than the tautomers from the point of view of a resonance assisted hydrogen bond (RAHB) effect [13]. Its acid dissociation given rise to anionic species may occur in aqueous phase but in the organic solvent used the two neutral tautomers are the major species present. A chemical quantum calculation showed that the *p*-quinone methide is the most stable form in gas phase. However, in both polar protic and non-polar solvents the *o*-quinone methide tautomer is predicted to be slightly favored in solution [12].

The emission decays of citrinin in solution of organic solvents are biexponential as illustrated by the decays in Fig. 6. The measured decay times in different solvents are reported in Table 1. The excited-state dynamics is described by two decay components of about 1 ns and 3–5 ns depending on the solvent. The first component corresponds to about 5 % of the entire decay weighted intensity. The small weight percent of the fast component recovered in the biexponential fitting would cause a doubt about the number of active decay components, but single exponential fitting resulted in unacceptable chi-square values (1.94, 1.49 and 1.79 in the case of citrinin in 2-propanol, acetonitrile and THF, respectively). Considering the tautomeric equilibrium described in Fig. 5, these results point out that an excited-state double proton transfer (ESDPT) should occur to convert the *o*-quinone methide into the *p*-quinone methide form. Such assumption would explain the large Stokes shift observed in absorption and emission maxima (see for instance Figs. 1, 2 and 3).

When citrinin traces are added to agarose, alginate, or polyvinylpyrrolidone hydrogel films, emission images, spectra as well as fluorescence decays can be measured by using confocal fluorescence microscopy techniques. In analytical concentration of 10^{-7}–10^{-8} mol/L (corresponding to 2.5–25 ng/mL) citrinin can be easily detected in hydrogel films as illustrated in the confocal fluorescence images of Fig. 7.

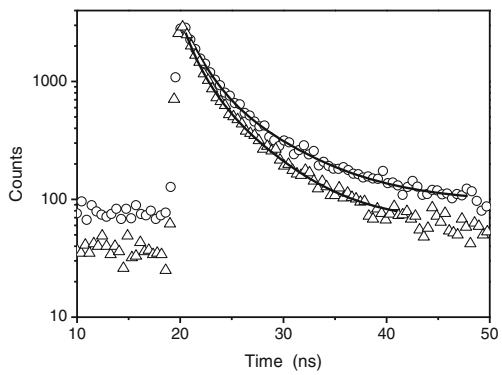

Fig. 9 Typical fluorescence decays of citrinin 1.0×10^{-7} M in agarose 1 % film (*white circle*) and in calcium alginate 0.1 % film (*white triangle*)

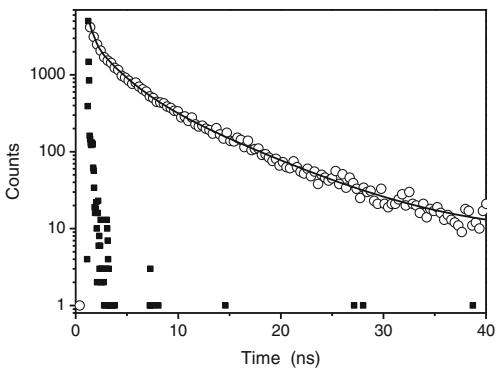

Fig. 10 Fluorescence decay of citrinin 1.0×10^{-8} M in PVP 2 % solution. Three exponential decay fitting resulted in decay times of 0.3, 2.2 and 7.3 ns with normalized amplitudes of 0.6, 0.3 and 0.1, respectively

The fluorescence images of the citrinin-containing agarose and alginate films produced micrometric emission spots indicating that such matrices are concentrating citrinin in small microdomains. In the case of a more hydrophilic polymer, like PVP, citrinin is dispersed over the whole matrix as shown in Fig. 7c given no clear emission spots. Typical emission spectra of citrinin in alginate film in different regions from the center of the emission spot to its border are plotted in Fig. 8.

In all prepared hydrogel films the emission maximum of citrinin was observed near 500 nm resembling the emission recorded in organic solvents (see emission in Figs. 1, 2 and 3).

The fluorescence decays of citrinin in the emissive spots dispersed in agarose and alginate were measured and typical decay traces are illustrated in Fig. 9. The decay analysis indicated again a biexponential relaxation of the fluorescence in both agarose and alginate hydrogel films. The fluorescence decays of citrinin in hydrogel films are clearly nonexponential and the fitting with two decay components gave acceptable chi-square values as reported in Table 2 and no improvement in the fitting was obtained with more one decay component.

In the case of agarose film, citrinin fluorescence decay is characterized by two components of 1.7 and 5.9 ns. In alginate film, the corresponding decay components have slightly lower values of 1.3 and 4.7 ns. Decay times recorded are averaged over different regions of the emission spots as reported in Table 2. Nevertheless, these values are close to the fluorescence decay times observed in organic solvents. However, contrasting with the previous decays in solution, in hydrogels films the fast component represents somewhat like 35 % of the decay intensity while in organic solvents such component corresponds to only 5 %. It means that the tautomeric equilibrium of citrinin changed upon dispersion in hydrogels films and the interconversion between tautomers by double proton transfer is controlled by the local polarity provided by the hydrogel films.

The almost homogeneous dispersion of citrinin in PVP hydrogel films precluded rapid decay measured in such systems using the confocal microscopy setup. However, the decay of citrinin in PVP 2 % 2-propanol solution was easier measured, and the result is displayed in Fig. 10. The decay observed is more complex than previous measurements and the excited-state dynamics could be well represented by a multiexponential decay function with three components (0.3, 2.2 and 7.3 ns with normalized amplitudes of 0.6, 0.3 and 0.1, respectively). The short lived component in the range of 300 ps not observed in the other systems may be related to deprotonation of citrinin producing the anion form in PVP solution with low emission. Such result is in agreement with the observation that citrinin fluorescence is maximized in pH close to 2.5, a condition where the formation of the anion is precluded.

Conclusions

The emission properties of the mycotoxin citrinin have been analyzed in different media. Citrinin showed complex fluorescence decay due to the presence of two tautomers in solution and due to a possible interconversion from excited-state double proton transfer (ESDPT). Fluorescence spectra and decay analysis could be used to recognize the presence of citrinin. Hydrogel films may be used to concentrate the toxin and microscopic regions with high emissive spots could be selected to indicate its presence. Further confirmation of citrinin could be performed by complementary analytical techniques using micro samples of the concentrated emissive spots.

Acknowledgments Financial support for fluorescence microscopy instrumentation was provided by FAPESP research grant 2011/18215-8. RGSB thanks to FAPESP for financial support (BIOTA/BIO*prospec*TA research grant 2010/50190-2). MHL thanks to FAPESP for a doctoral fellowship and KJ thanks to CAPES for a MSc scholarship. We thank to Professor Dr Johan Hofkens and Dr Kris P. F. Janssen for the use of SIS image software from the MDS Laboratory of the Department of Chemistry, Katholieke Universiteit Leuven.

References

1. Xu B, Jia X, Gu L, Sung C (2006) Review on the qualitative and quantitative analysis of the mycotoxin citrinin. Food Control 17:271–285
2. Nigovic B, Sertic M, Mornar A (2013) Simultaneous determination of lovastatin and citrinin in red yeast rice supplements by micellar electrokinetic capillar chromatography. Food Chem 138:531–538
3. Dohanal V, Pavliková L, Kuca K (2010) Rapid and sensitive method for citrinin determination using high-performance liquid chromatography with fluorescence detection. Anal Lett 43:786–792
4. Vázquez BI, Fente C, Franco CM, Quinto E, Cepeda A, Prognon P (1997) Rapid semi-quantitative fluorimetric determination of citrin in fungal cultures isolated from cheese and cheese factories. Lett Appl Microbiol 24:397–400
5. Li Y, Wu H, Guo L, Zheng Y, Guo Y (2012) Microsphere-based flow cytometric immunoassay for the determination of citrinin in red yeast rice. Food Chem 134:2540–2545
6. Guo BY, Wang S, Ren B, Li X, Qin F, Li J (2010) Citrinin selective molecularly imprented polymers for SPE. J Sep Sci 33:1156–1160
7. Zhou Y, Chen J, Dong L, Lu L, Chen F, Hu D, Wang X (2012) A study of fluorescence properties of citrin in β-cyclodextrin aqueous solution and different solvents. J Luminescence 132:1437–1445
8. Devi P, D'Souza L, Kamat T, Rodrigues C, Naik CG (2009) Batch culture fermentation of Penicillium chrysogenum and a report on the isolation, purification, identification and antibiotic activity of citrinin. Indian J Mar Sci 38:38–44
9. Hajjaj H, Klaebe A, Loret MO, Goma G, Blanc PG, Francois J (1999) Biosynthetic pathway of citrinin in the filamentous fungus Monascus ruber as revealed by ^{13}C nuclear magnetic resonance. Appl Environ Microbiol 65:311–314
10. Destro R (1991) Proton transfer in the solid state:thermodynamic parameters from an X-ray study in the temperature range 20–293 K. Chem Phys Letters 181:232–236

11. Poupko R, Luz Z, Destro R (1997) Carbon-13 NMR of citrinin in the solid state and in solutions. J Phys Chem A 101:5097–5102
12. Appel M, Moravec D, Bosma WB (2012) Quantum chemical study of the structure and properties of citrinin. Mol Simul 38:284–292
13. Bertolasi V, Gilli P, Ferretti V, Gilli G (1997) Intramolecular O-H O hydrogen bonds assisted by resonance. Correlation between crystallographic data and ^{1}H NMR chemical shifts. J Chem Soc Perkin Trans 2:945–952